Quasi-one-dimensional superconductivity above 300 K and quantum phase slips in individual carbon nanotubes

Guo-meng Zhao*
Department of Physics, Texas Center for Superconductivity and Advanced Materials, University of Houston, Houston, Texas 77204, USA

A great number of the existing data for electrical transport, the Altshuler Aronov Spivak and Aharonov Bohm effects, as well as the tunneling spectra of individual carbon nanotubes can be well explained by theories of the quantum phase slips in quasi-one-dimensional superconductors. The existing data consistently suggest that the mean-field superconducting transition temperature T_{c0} in both single-walled and multi-walled carbon nanotubes could be higher than 600 K. The quantum phase slip theories naturally explain why the on-tube resistances in the closely packed nanotube bundles or in the individual multi-walled nanotubes with large diameters approach zero at room temperature, while a single tube with a small diameter has a substantial resistance.

The discovery of high-temperature superconductivity at about 40 K in electron-doped C_{60} [1] suggests that the electron-lattice coupling with high-energy phonons in this graphite-related material should be strong. Otherwise, T_c could not be so high because the Coulomb pseudopotential μ^* in C_{60} should be larger than 0.2 due to a small Fermi energy ($\sim$ 0.2 eV) and a large phonon energy ($\sim$ 0.2 eV) [1]. The strong electron-phonon coupling in C_{60} may arise from the finite curvature of the graphite sheets, that leads to hybridization of σ, π, σ^* and π^* states [2] and thus enhances the electron-phonon coupling. Similarly, the finite curvature of the carbon nanotubes (CNTs) produces a stronger electron-phonon coupling compared to their zero curvature counterpart, graphene. Moreover, the CNTs have a quasi-one or quasi-two-dimensional electronic structure. It was shown that in multi-layer systems such as cuprates and multi-walled nanotubes (MWNT), high-temperature superconductivity can occur due to an attraction of the carriers in the same conducting layer via exchange of virtual plasmons in neighboring layers [3]. Similarly, exchange of undampled acoustic plasmon modes in quasi-one-dimensional systems can also lead to high-temperature superconductivity [4]. Thus, the CNTs should have a much higher mean-field superconducting transition temperature T_{c0} than doped C_{60} due to the presence of strong electron-phonon and electron-plasmon coupling. Zhao *et al.* [5] have recently argued for the existence of superconductivity above 600 K in MWNT ropes. In order to confirm this claim, it is helpful to show the zero-resistance state at room temperature in the nanotubes. However, one should also consider the quasi-one-dimensional nature of the nanotubes, which may lead to a finite on-tube resistance below T_{c0}.

Here we extensively analyze the existing data for electrical transport, magnetoresistance and tunneling spectra of both single-walled and multi-walled carbon nanotubes. The data can be well explained by theories of quantum phase slips (QPS) in one-dimensional superconductors. Moreover, the existing data consistently suggest that the mean-field superconducting transition temperature T_{c0} in both single-walled and multi-walled carbon nanotubes could be higher than 600 K.

It is known that superconducting fluctuations in one-dimensional (1D) superconductors play an essential role in the resistive transition. Slightly below superconducting transition temperature T_{c0}, 1D superconductors have a finite resistance due to thermally activated phase slips (TAPS) [6]. A number of experiments have also demonstrated a large resistance well below T_{c0} in thin superconducting wires [7,8,9,10]. Further, a crossover to an insulating state has been observed in ultrathin PbIn wires with diameters of the order of 10 nm [7,9] as well as in ultrathin wires of MoGe [10].

Theories based on the quantum phase slips can explain the finite resistance in 1D superconductors [8,11]. Essentially, the phase slips at low temperatures are related to the macroscopic quantum tunneling (MQT), which allows the phase of the superconducting order parameter to fluctuate between zero and 2π at some points along the wire, resulting in voltage pulses. For a single electron, the scatterings by impurities, phonons and other electrons can change the phase of the electron. The uncertainty in the phase of the single electron due to scattering leads to localization of the electron. By analogy, the uncertainty in the phase of the Cooper pairs due to QPS results in localization of the Cooper pairs and thus a non-zero resistance [10]. The QPS tunneling rate is proportional to $\exp(-S_{QPS})$, where S_{QPS} in clean superconductors is very close to the number of transverse channels N_{ch} in the limit of weak damping (see below). If the number of the transverse channels N_{ch} is small, the QPS tunneling rate is not negligible, leading to a non-zero resistance at low temperatures. For a single-walled nanotube (SWNT), N_{ch} = 2, implying a large QPS tunneling rate and thus a large resistance even if it

is a superconductor. For MWNTs with several superconducting layers adjacent to each other, the number of the transverse channels will increase substantially, resulting in the large suppression of the QPS if the Josephson coupling among the layers is strong. If two superconducting tubes are closely packed together to effectively increase the number of the channels, one would find a small on-tube resistance at room temperature if the constituent tubes have a mean-field T_{c0} well above room temperature. This can naturally explain why a single MWNT with a diameter d of about 17 nm has a finite on-tube resistance at room temperature [12,13] while a bundle consisting of two MWNT tubes has a negligible on-tube resistance [14].

There are thermally activated phase slips (TAPS) and quantum phase slips in a thin superconducting wire. A theory developed by Langer, Ambegaokar, McCumber and Halperin [6], describes phase slips which occur via thermal activation. The resistance due to the TAPS is given by [15]

$$R_{TA} = R_Q \frac{\hbar\Omega}{2k_BT} \exp(-\Delta F_\circ/k_BT), \tag{1}$$

where $R_Q = h/2e^2$ =12.9 kΩ is the resistance quantum and the attempt frequency Ω is given by [6]

$$\Omega = \frac{\sqrt{3}}{2\pi^{3/2}} \frac{L}{\xi} \sqrt{\frac{\Delta F_\circ}{k_BT}} \frac{1}{\tau}. \tag{2}$$

Here L is the length of the wire, ξ is the coherence length, and $\hbar/\tau = (8/\pi)k_B(T_{c0} - T)$. The barrier energy $\Delta F_\circ$ is

$$\Delta F_\circ = \frac{8\sqrt{2}}{3} \frac{H_c^2}{8\pi} A\xi, \tag{3}$$

where $H_c^2/8\pi$ is the condensation energy and A is the cross-sectional area of the wire. The condensation energy is equal to $N(0)\Delta^2/2$ within the BCS theory, where $N(0)$ is the average density of states near the Fermi level over the energy scale of the superconducting gap Δ. For a metallic SWNT with N_{ch} =2, $N(0)A = 4/3\pi a_{C-C}\gamma_\circ$ (Ref. [16]), $\hbar v_F = 1.5a_{C-C}\gamma_\circ$ (Ref. [17]), where $\gamma_\circ$ is the hopping integral and a_{C-C} is the bonding length. Using $\xi = \hbar v_F/\pi\Delta$, $\hbar/\tau = (8/\pi)k_BT_{c0}$, $2\Delta/k_BT_{c0}$ =3.52, and the above relations, one can readily show that $\Delta F_\circ\tau/\hbar \simeq 0.13N_{ch}$ and $\Delta F_\circ/\Delta \simeq 0.19N_{ch}$. For MWNTs with N_l superconducting layers, $\Delta F_\circ\tau/\hbar = 0.26N_l$ and $\Delta F_\circ/\Delta = 0.38N_l$.

It was shown that the TAPS is significant only at temperatures very close to and below T_{c0} [6]. At lower temperatures, the finite resistance is caused by MQT and is given by [8].

$$R_{MQT} = \beta_1 R_Q \frac{L}{\xi} \sqrt{\frac{\beta_2 \Delta F_\circ \tau}{\hbar}} \exp(-\beta_2 \Delta F_\circ\tau/\hbar), \tag{4}$$

where β_1 and β_2 are constants, depending on the damping strength. When the damping increases, β_2 decreases.

Substituting $\Delta F_\circ\tau/\hbar = 0.26N_l$ into Eq. 4, we find that

$$R_{MQT} = \beta_1 R_Q \frac{L}{\xi} \sqrt{0.26\beta_2 N_l} \\ \exp(-0.26\beta_2 N_l). \tag{5}$$

From Eq. 5, one can see that $S_{QPS} \simeq 2N_l$ in the limit of weak damping where $\beta_2 = 7.2$ (Ref. [8]). For a stronger damping, β_2 is reduced so that $S_{QPS} < 2N_l$. Moreover, in the dirty limit, S_{QPS} will be further reduced [11] such that $S_{QPS} << 2N_l$. For a SWNT, $N_l = 1$ so that a large QPS and a nonzero resistance is expected below the mean-field superconducting transition temperature. If several superconducting SWNTs are closely packed to ensure an increase in the number of channels, the QPS would be substantially reduced. This can explain why the on-tube resistance is appreciable at room temperature for a single SWNT [18,19] while the resistance at room temperature is very small for a bundle consisting of two strongly coupled SWNTs [13]. For a MWNT with $d = 40$ nm, there is a total of 27 metallic layers, that is, $N_l = 27$ (Ref. [20]). This implies that the QPS in this single MWNT should be strongly suppressed according to Eq. 5. Indeed, this MWNT has nearly zero on-tube resistance at room temperature over a length of 4 μm (Ref. [20]).

More rigorous approach quantifying the QPS in quasi-1D superconductors [11] suggests that S_{QPS} depends not only on the quantity $\Delta F_\circ\tau/\hbar$ but also on the normal-state conductivity σ ($S_{QPS} \propto \sigma^{2/3}$). Therefore, one can very effectively suppress the QPS and the resistance below T_{c0} by reducing the normal-state resistivity. It was shown that the electron backscattering from a single impurity with long range potential is nearly absent in metallic SWNTs while this backscattering becomes significant for doped semiconducting SWNTs [21]. This implies that the QPS in doped metallic SWNTs will be significantly smaller than that in doped semiconducting SWNTs if both systems become superconducting by doping.

Now we discuss the temperature dependence of the resistance observed in nanotubes. Fig. 1a shows the temperature dependence of the four-probe resistance for a single MWNT with $d = 17$ nm, which is reproduced from Ref [12]. It is remarkable that the resistance increases with decreasing temperature, but saturates at low temperatures. This unusual temperature dependence is very difficult to be explained consistently in terms of the conventional theory of transport [12]. However, a theory based on the QPS in 1D superconductors can naturally explain this unusual behavior. It was shown that [11], the resistance $R \propto T^{3\mu-2}$ for $k_BT >> \Phi_\circ I/c$, and R becomes independent of temperature and is proportional to $I^{3\mu-2}$ for $k_BT << \Phi_\circ I/c$. Here $\Phi_\circ$ is the quantum flux, c is the speed of light, I is the current, and μ is a quantity

that characterizes the ground state; the zero-temperature resistance can approach zero when $\mu > 2$, and is finite when $\mu < 2$. The crossover from the power-law behavior to the temperature independent behavior takes place at $T \sim \Phi_\circ I/ck_B$. For example, the crossover temperature is about 7 K for $I = 50$ nA. When $\mu < 1.5$, R increases with decreasing temperature (semiconducting behavior), while for $\mu > 1.5$, R decreases with decreasing temperature (metallic behavior). Only if the QPS are strongly suppressed, can a zero or negligible resistance state be realized below T_{c0}.

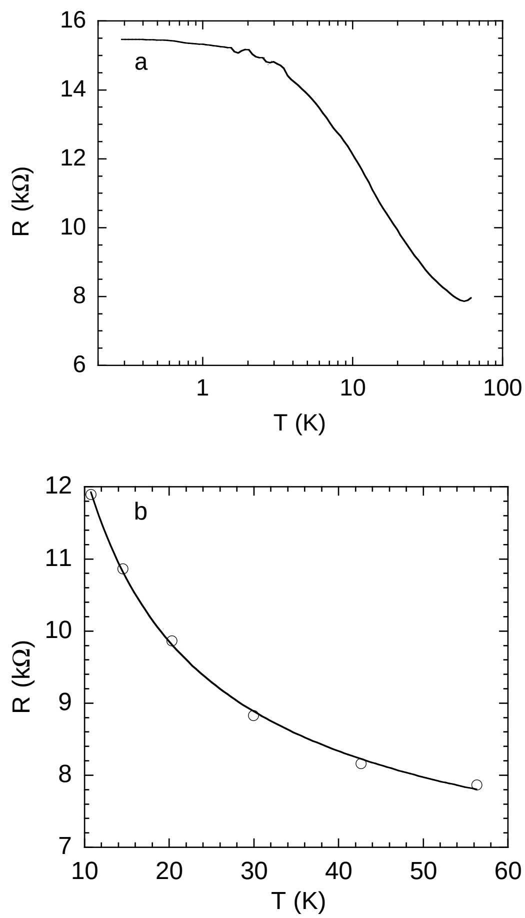

FIG. 1. a) The temperature dependence of the four-probe resistance for a single MWNT with $d = 17$ nm, which is reproduced from Ref [12]. b) The temperature dependence of the resistance over 10-60 K, which is fitted by $R(T) = R_{ct} + aT^p$. The fitting parameters: $R_{ct} = 5.6(5)\ k\Omega$, $p = -0.65(9)$, and $a = 29(4) k\Omega K^{0.65}$.

From the QPS theory, we can show that for $\Phi_\circ I/ck_B << T << T_{c0}$, the four-probe resistance $R(T)$ is

$$R(T) = R_{ct} + aT^p, \tag{6}$$

where R_{ct} is the tunneling resistance and $p = 3\mu - 2$. The tunneling resistance is given by $R_{ct} = R_Q/tN_{ch}$, where t is the transmission coefficient ($t \leq 1$).

In Fig. 1b, we fit the resistance of the MWNT by Eq. 6. The best fit gives $R_{ct} = 5.6(5)$ kΩ, $p = -0.65(9)$, and $a = 29(4)\ k\Omega K^{0.65}$. At zero temperature $R(0) = R_s + R_{ct}$, where R_s is the on-tube saturation resistance at zero temperature. The value of R_{ct} (5.6 kΩ) and the value of $R(0)$ (15.3 kΩ) suggest that the on-tube saturation resistance of the tube is 9.7 kΩ.

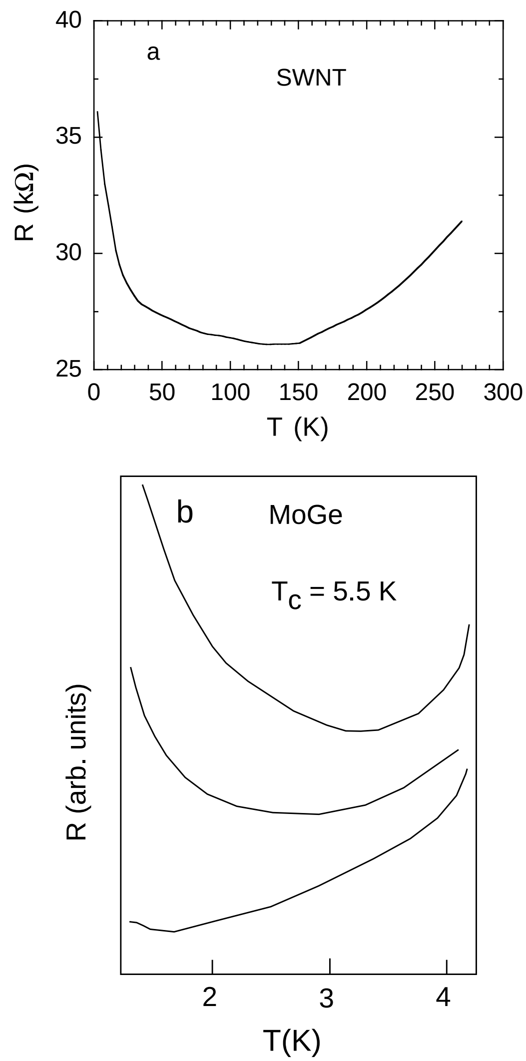

FIG. 2. a) Temperature dependence of the resistance for a SWNT. The data are extracted from Ref. [18]. b) Temperature dependence of the resistance for three ultrathin MoGe wires. The curves are smoothed from the original plot of Ref. [10].

From the value of R_{ct} for the MWNT, we can estimate the transmission coefficient t. As discussed below, the high bias transport measurements in MWNTs [22] suggest that there is a total of 14 conducting layers in a MWNT with $d = 14$ nm, and that the number of the

conducting layers is nearly proportional to d. Then, the MWNT with $d = 17$ nm should have about 17 conducting layers. Moreover, the beautiful experiment reported by de Pablo *et al.* [20] indicates that each conducting layer contributes 1 transverse channel to electrical transport. If one takes $N_{ch} = 17$ for the MWNT with d= 17 nm, one finds $t = 0.135$. This suggests that the tunneling is far from being ideal, which may arise from non-Ohmic contacts. We should mention that each layer should contribute 2 channels if there were no interlayer coupling. However, it has been shown that the interlayer coupling can significantly modify the electronic states near the Fermi level, leading to the modulation in the number of channels between 1 and 3 for each layer (the average number of channels over an energy scale of 0.1 eV remains 2 for each layer) [23,24].

In Fig. 2a, we plot the temperature dependence of the resistance for a single SWNT. The data are extracted from Ref. [18]. It is interesting that the temperature dependence of the resistance in the single-walled nanotube is similar to that found for ultrathin wires of MoGe superconductors [10], facsimile of which is reproduced in Fig. 2b. The characteristic temperature T^* corresponding to the local resistance minimum depends on the resistance in the normal state. It appears that T^* decreases with decreasing resistance. The resistance at low temperatures could be smaller or larger than that in the normal state. By comparing Fig. 2a and Fig. 2b, one might infer that the mean-field T_{c0} of this nanotube is well above 270 K.

From the single-particle tunneling spectrum obtained through two high-resistance contacts (see Fig. 1b of Ref. [19]), we can clearly see a pseudo-gap feature which appears at an energy of about 220 meV. The pseudo-gap feature should be related to the superconducting gap rather than to the Luttinger-liquid behavior, as shown below. Considering the broadening of the gap feature due to the large QPS and the double tunneling junctions in series, we estimate the superconducting gap Δ to be about 100 meV. Scanning tunnelling microscopy and spectroscopy [25] on individual single-walled nanotubes also show the pseudo-gap features with $\Delta \simeq 100$ meV in doped metallic SWNTs (the Fermi level E_F is about 0.2 eV below the top of the valence band). Using $k_B T_{c0} = \Delta/1.76$, we find $T_{c0} \simeq 660$ K. It is interesting to note that the pseudo-gap feature could also be explained by Luttinger-liquid theory [26,27] assuming that the Luttinger parameter is far below the free fermionic value of 1. The fact that the pseudo-gap feature is seen only in heavily doped metallic chirality tubes [25] but not in undoped or lightly doped armchair tubes [28] may rule out the Luttinger-liquid explanation since theory [27] does not expect that Luttinger-liquid behavior should disappear in undoped or lightly doped armchair tubes with finite lengths.

Now let us explain one of the most remarkable features observed in carbon nanotubes. At large biases, the current saturates at 19-23 μA in SWNTs [19]. The current saturation has been explained as due to the backscattering of the zone-boundary optical phonons [19]. However, the deduced mean free path for phonon backscattering is one order of magnitude smaller than the expected one from the tight-binding approximation [19]. Further, the $I-V$ characteristic observed in SWNTs is temperature independent for $V > 0.1$ V (Ref. [19]) while the calculated $I-V$ characteristic within this mechanism should strongly depend on temperature especially in the low-bias range [29].

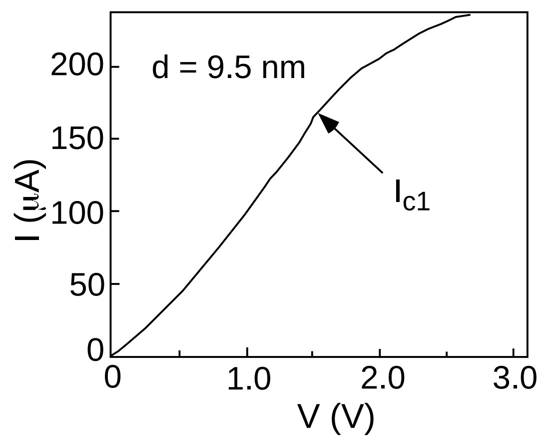

FIG. 3. The $I-V$ characteristic observed in a MWNTwith $d = 9.5$ nm. The figure is reproduced from Ref. [22].

Alternatively, we explain the $I-V$ characteristics of both SWNTs and MWNTs [19,22] in terms of quasi-1D superconductivity. Essentially, the $I-V$ characteristics of both SWNTs and MWNTs [19,22] are similar to that observed in ultrathin PbIn superconducting wires (see Fig 8 of Ref. [9]). Fig. 3 shows the $I-V$ characteristic observed in a MWNT with $d = 9.5$ nm. The figure is reproduced from Ref. [22]. When the applied current is below the lower critical current I_{c1}, the QPS are negligible so that the intrinsic on-tube resistance is much smaller than the normal-state resistance, and V depends on I rather linearly. The slope dV/dI is equal to the sum of the on-tube resistance and the contact resistance. When the applied current increases slightly above I_{c1}, the on-tube resistance rises rapidly towards the normal-state value due to the large QPS, leading to the dissipation that can burn the tube. If the tube is not burned, the current tends to be saturated before the tube is completely driven into the normal state. The saturation current is close to the mean-field critical current I_c in the absence of defects. Since phase slips initially occur near normal regions located around defects in the sample, we expect that I_{c1} should strongly depend on the density of

defects and thus on the normal-state resistivity. From Fig. 3, one can see that $I_{c1} \leq 0.75 I_c$.

According to the BCS theory, the mean-field critical current in the clean limit is given by [15]

$$I_c(T) = e n_s(T) A \frac{\Delta(T)}{\hbar k_F}. \quad (7)$$

The superfluid density $n_s(T) = n\lambda^2(0)/\lambda^2(T)$, and the normal-state carrier density $n = 2N(0)E_F = 2N(0)\hbar v_F k_F = 4k_F/A\pi$. Here we have used the relations: $N(0)A = 4/3\pi a_{C-C}\gamma_\circ$, and $\hbar v_F = 1.5 a_{C-C}\gamma_\circ$, as well as $E_F = \hbar v_F |k_F|$. Substituting the above relations into Eq. 7 yields

$$I_c(T) = 7.04 N_l \frac{k_B T_{c0}}{eR_Q} \frac{\lambda^2(0)}{\lambda^2(T)} \frac{\Delta(T)}{\Delta(0)}, \quad (8)$$

with $I_c(0) = 7.04 N_l k_B T_{c0}/eR_Q$. Here $\lambda^2(0)/\lambda^2(T)$ follows the BCS prediction, and $\Delta(T) = \Delta(0)\tanh(1.6\sqrt{T_{c0}/T - 1})$, which is very close to that predicted by the BCS theory. The critical current i_c per superconducting layer is then given by

$$i_c(T) = 7.04 \frac{k_B T_{c0}}{eR_Q} \frac{\lambda^2(0)}{\lambda^2(T)} \frac{\Delta(T)}{\Delta(0)}. \quad (9)$$

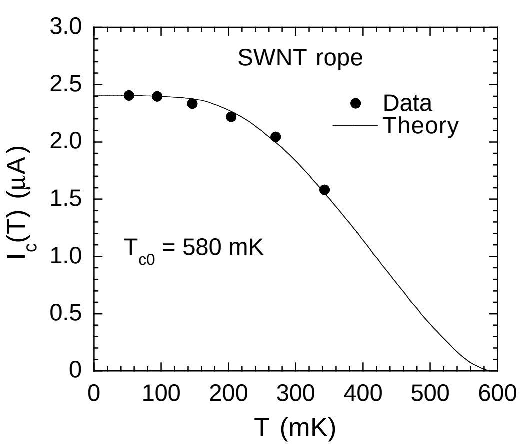

FIG. 4. The critical current $I_c(T)$ for a SWNT rope. The data are extracted from Ref. [30]. The solid line is the calculated curve using Eq. 8 and T_{c0} = 580 mK.

For a SWNT rope, the resistance starts to drop below about 550 mK and reaches a value R_r = 74 Ω at low temperatures [30]. The data are consistent with quasi-1D superconductivity with $T_{c0} \simeq$ 550 mK and $N_l = R_Q/2R_r$ = 87 (Ref. [30]). Substituting these numbers into the expression: $I_c(0) = 7.04 N_l k_B T_{c0}/eR_Q$, we obtain $I_c(0)$ =2.25 μA, in excellent agreement with the measured $I_c(0)$ = 2.41 μA, as seen from Fig. 4. The solid line in Fig. 4 is the calculated curve using Eq. 8 and T_{c0} = 580 mK. It is striking that the data are in quantitative agreement with theory. We should mention that very low superconductivity in the SWNT rope may be due to the fact that the tubes are very lightly doped. The very high normal-state resistance (830 kΩ/μm) per tube [30] suggests that the Fermi level must be very close to the top of the valence band where the Fermi velocity must be significantly reduced due to the opening of a small gap in non-armchair metallic tubes.

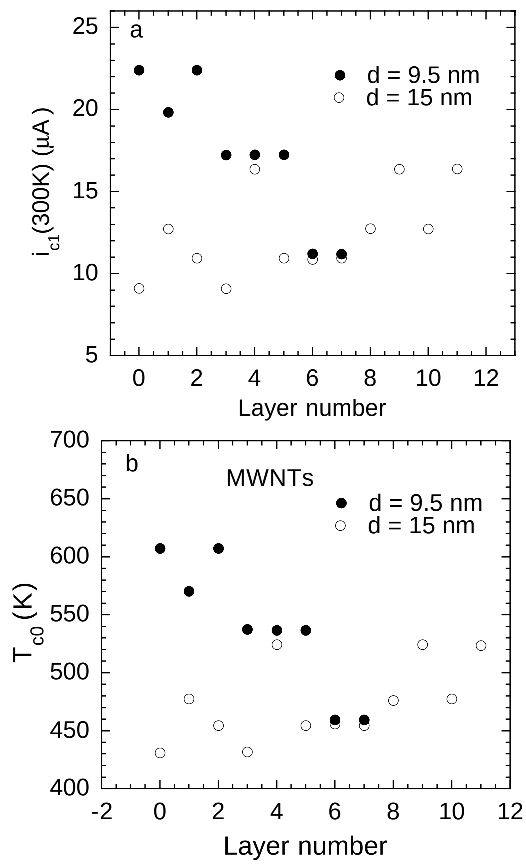

FIG. 5. a) The critical currents i_c's at 300 K for the individual superconducting layers in a MWNT with d = 9.5 nm and in a MWNT with d = 15 nm. The data are extracted from Ref. [22]. b) The mean-field critical temperature T_{c0}'s of individual superconducting layers in the MWNTs with d = 9.5 nm and 15 nm, respectively. The T_{c0}'s are calculated using Eq. 9 and assuming $i_c = i_{c1}$.

In Fig. 5a, we show the critical currents i_{c1}'s at 300 K for individual superconducting layers in a MWNT with d = 9.5 nm and in a MWNT with d = 15 nm. The data are extracted from Ref. [22]. The layer number starts from 0 that corresponds to the outermost superconducting layer. For d = 9.5 nm the i_c tends to decrease with decreasing the diameter of the layer, while for d = 15 nm the tendency is just the opposite. Plotted in Fig. 5b is the mean-field critical temperature T_{c0}'s of individual superconducting layers in the MWNTs, which are calculated using Eq. 9 and assuming $i_c = i_{c1}$. From the

discussion associated with Fig. 3, it is clear that the calculated T_{c0}'s are underestimated because i_c should always be larger than i_{c1}. One can see that T_{c0} varies from 430 K to 610 K, in good agreement with the independent resistance data [5]. This broad variation in T_{c0} suggests that T_{c0} depends on doping and on the diameters of tubes. Indeed, a lower T_{c0} value of about 300 K can be inferred from the temperature dependence of the resistance in a single MWNT with $d \simeq 12$ nm, which is reproduced from Ref. [31] and shown in Fig. 6. It is likely that this MWNT is not optimally doped so that the T_{c0} of the tube is much lower than the one (> 600 K) for optimally doped MWNTs.

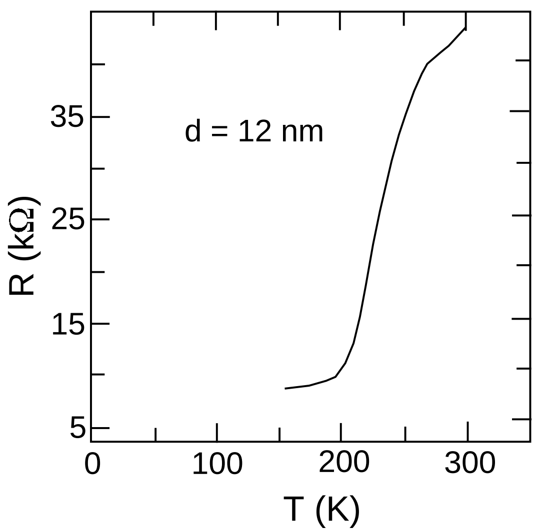

FIG. 6. The temperature dependence of the resistance in a single MWNT with $d \simeq 12$ nm, which is reproduced from Ref. [31]. The sudden drop in the resistance below 300 K can be explained in terms of quasi-1D superconductivity with $T_{c0} \simeq 300$ K. The non-zero resistance below 200 K arises from phase slips and from the contact resistance R_{ct} discussed above.

Now we turn to discuss the Aharonov Bohm (AB) effect, which has been observed in MWNTs when the magnetic field is applied along the tube-axis direction [32,12]. The magnetoresistance measurements showed pronounced resistance oscillations as a function of magnetic flux. The oscillation period was found to be about $\Phi_\circ$ ($= hc/2e$) if one assumed that only the outermost layer is involved in conduction [32,12]. The result could be consistent with the Altshuler Aronov Spivak (AAS) effect, which arises from quantum interference of two counter-propagating closed diffusive electron trajectories [34]. On the other hand, a period of $2\Phi_\circ$ should have been observed if the phase coherence length of single particles is reasonably larger than πd (the AB effect for the single particle density of states [33]). If the phase coherence length L_ϕ deduced from experiment (e.g., $L_\phi \sim 300$ nm $>> \pi d$ in one of the MWNTs [32]) were related to that for single particles, one would have observed the AB effect. However, such an effect has never been observed [32,12]. Therefore, this contradiction cannot be resolved if the conduction carriers were single particles.

We can resolve the above discrepancy if we assume that the conduction carriers are Cooper pairs in the limit of weak localization (WL). As we discussed above, the uncertainty in the phase of Cooper pairs due to the large QPS could lead to weak localization of the Cooper pairs [10]. In many situations, a Cooper pair can be equivalent to a particle with a charge of $2e$. This simplification suggests that the WL theory for single particles should be applicable for Cooper pairs upon replacing e with $2e$. With this interpretation, we can readily find that the magnetic-flux period of the AAS effect for the Cooper pairs is $\Phi_\circ/2$, and that the AB effect for the single particle density of states should be absent if the phase coherence length for single particles is less than πd.

In fact, the assumption that only the outermost layer is conducting [12,32] is not justified. As we discussed above, 14 and 27 layers are involved in conduction in MWNTs with $d = 14$ nm and 40 nm, respectively. Further, the resistance at 1.3 K for a MWNT with $d = 13$ nm is 2.45 kΩ (Ref. [32]). The value of the resistance suggests that there are at least 6 transverse channels and 6 conducting layers which are involved in conduction. The average magnetic flux sensed by the carriers in all the conducting layers should be $B\pi(r_{out}^2 + r_{in}^2)/2$, where r_{out} and r_{in} are the radii of the outermost and innermost conducting layers, respectively, and B is the magnetic field. We can calculate r_{in} using the relation $r_{in} = r_{out} - 0.34(N_l - 1)$ nm. For the MWNT with $d = 17$ nm, $N_l = 17$ (see above), leading to $r_{in} = 3.06$ nm. From the measured magnetic-field period of 8.2 T in the MWNT [12], we find that the magnetic-flux period is $0.51\Phi_\circ$, in quantitative agreement with the thesis that the charge carriers are Cooper pairs with a finite phase coherence length due to the QPS.

In summary, the theories based on the QPS in 1D superconductors can quantitatively explain a large number of the existing data for electrical transport, the AAS and AB effects, as well as tunneling spectra of both SWNTs and MWNTs. The existing data consistently suggest that the mean-field superconducting transition temperature T_{c0} in both single-walled and multi-walled carbon nanotubes could be as high as 600 K. It is interesting that the energy gap (pairing energy) in the carbon nanotubes is very close to that for deeply underdoped cuprates, which would exhibit phase-coherent superconductivity above room temperature if one could increase the superfluid density. The high pairing energy in both cuprates and carbon nanotubes may arise from strong electron-phonon coupling and strong electron-plasmon interaction. The possibility of phase-coherent supercon-

ductivity above room temperature in a single MWNT with $d = 40$ nm [20] is due to the fact that the effective mass for the graphite-related materials is more than two orders of magnitude smaller than in the cuprates, and that the QPS are strongly suppressed due to the large number of transverse channels.

Acknowledgment: I thank Dr. Pieder Beeli for his critical reading and comments on the manuscript. The author acknowledges financial support from the State of Texas through the Texas Center for Superconductivity and Advanced Materials at the University of Houston where some of the work was completed.

Correspondence should be addressed to gmzhao@uh.edu.

---

[1] O. Gunnarsson, Rev. Mod. Phys. **69**, 575 (1997).
[2] X. Blase, L. X. Benedict, E. L. Shirley, and S. G. Louie, Phys. Rev. Lett. **72**, 1878 (1994).
[3] S. M. Cui and C. H. Tsai, Phys. Rev. B **44**, 12500 (1991).
[4] Y.C. Lee and B. S. Mendoza, Phys. Rev. B **39**, 4776 (1989).
[5] G. M. Zhao and Y. S. Wang, cond-mat/0111268.
[6] J. S. Langer and V. Ambegaokar, Phys. Rev. **164**, 498 (1967); D. E. McCumber and B. I. Halperin, Phys. Rev. B **1**, 1054 (1970).
[7] N. Giordano and E. R. Schuler, Phys. Rev. Lett. **63**, 2417 (1989).
[8] N. Giordano, Phys. Rev. B **41**, 6350 (1990).
[9] N. Giordano, Phys. Rev. B **43**, 160 (1991).
[10] A. Bezryadin, C. N. Lau, and M. Tinkham, Nature (London) **404**, 971 (2000).
[11] A. D. Zaikin, D. S. Golubev, A. van Otterlo, and G. T. Zimnyi, Phys. Rev. Lett. **78**, 1552 (1997).
[12] C. Schönenberger, A. Bachtold, C. Strunk, J.-P. Salvetat, L. Forro, Appl. Phys. A bf 69, 283 (1999).
[13] A. Bachtold, M. S. Fuhrer, S. Plyasunov, M. Forero, E. H. Anderson, A. Zettl, and P. L. McEuen, Phys. Rev. Lett. **84**, 6082 (2000).
[14] S. Frank, P. Poncharal, Z. L. Wang, Walt A. de Heer, Science **280**, 1744 (1998).
[15] M. Tinkham, Introduction to Superconductivity (McGraw-Hill, 1996).
[16] Stephan Roche and Riichiro Saito, Phys. Rev. B **59**, 5242 (1999).
[17] J. W. Mintmire and C. T. White, Phys. Rev. Lett. **81**, 2506 (1998).
[18] H. T. Soh, C. F. Quatea, A. F. Morpurgo, C. M. Marcusb, J. Kong and H. J. Dai, Appl. Phys. Lett. **75**, 627 (1999).
[19] Z. Yao, C. L. Kane, and C. Dekker, Phys. Rev. Lett. **84**, 2941 (2000).
[20] P. J. de Pablo, E. Graugnard, B. Walsh, R. P. Andres, S. Datta, and R. Reifenbergera, Appl. Phys. Lett. **74**, 323 (1999).
[21] Stephan Roche, Francois Triozon, and Angel Rubio, Appl. Phys. Lett. **79**, 3690 (2001).
[22] Philip G. Collins, M. Hersam, M. Arnold, R. Martel, and Ph. Avouris, Phys. Rev. Lett. **86**, 3128 (2001); Philip G. Collins, Michael S. Arnold, Phaedon Avouris, Science **292**, 706 (2001).
[23] Young-Kyun Kwon and David Tomanek, Phys. Rev. B **58**, R16001 (1998).
[24] S. Sanvito, Y.-K. Kwon, D. Tomanek, and C. J. Lambert, Phys. Rev. Lett. **84**, 1974 (2000).
[25] Jeroen W. G. Wildoer, Liesbeth C. Venema, Andrew G. Rinzler, Richard E. Smalley, and Cees Dekker, Nature (London) **391**, 59 (1998).
[26] M. Bockrath, D. H. Cobden, J. Lu, A. G. Rinzler, R. E. Smalley, L. Balents, and P. L. McEuen, Nature (London) **397**, 598 (1999).
[27] C. Kane, L. Balents, and M. P. A. Fisher, Phys. Rev. Lett. **79**, 5086 (1997).
[28] M. Ouyang, J. L. Huang, C. L. Cheung, and C. M. Lieber, Science **292**, 702 (2001).
[29] G. D. Mahan and G. S. Canright, Phys. Rev. B **35**, 4365 (1987).
[30] M. Kociak, A.Yu. Kasumov, S. Gueron, B. Reulet, I. I. Khodos, Yu. B. Gorbatov, V. T. Volkov, L. Vaccarini, and H. Bouchiat, Phys. Rev. Lett. **86**, 2416 (2001).
[31] T. W. Ebbesen, H. J. Lezec, H. Hiura, J. W. Bennett, H. F. Ghaemi, and T. Thio, Nature (London) **382**, 54 (1996).
[32] A. Bachtold, C. Strunk, J. P. Salvetat, J. M. Bonard, L. Forro, T. Nussbaumer, and C. Schönenberger, Nature (London) **397**, 673 (1999).
[33] S. Roche, G. Dresselhaus, M. S. Dresselhaus, and R. Saito, cond-mat/0005070.
[34] A. G. Aronov and Y. V. Sharvin, Rev. Mod. Phys. **59**, 755 (1987).